

## Electronic Supplementary Information (ESI): Particle Emissions of a Heavy-Duty Engine Fueled with Polyoxymethylene Dimethyl Ethers (OME)

Alexander Daniel Gelner<sup>a</sup>, Dieter Rothe<sup>b</sup>, Carsten Kykal<sup>c</sup>, Martin Irwin<sup>d</sup>, Alessandro Sommer<sup>a</sup>,  
Christian Pastötter<sup>b</sup> and Georg Wachtmeister<sup>a</sup>

<sup>a</sup> Technical University of Munich, Institute of Internal Combustion Engines, Schragenhofstraße 31, 80992 Munich, Germany.

<sup>b</sup> MAN Truck & Bus SE, Vogelweierstraße 33, Nuremberg, Germany.

<sup>c</sup> TSI GmbH, Neuköllner Straße 4, 52068 Aachen, Germany.

<sup>d</sup> Catalytic Instruments GmbH & Co. KG, Zellerhornstraße 7, 83026 Rosenheim.

### Measurement methods of OME values

Table 1. Determined values of OME and the respective measurement method

	Value	Method
Cetane number	68.8	DIN EN 17155 :2018
Oxygen content in % (w/w)	45.0	DIN 51732 :2014 mod..
Sulfur content in mg/kg	< 5	DIN EN ISO 20884 :2011
Lower heating value in MJ/kg	19.21	DIN 51900-2 :2003 mod.
Density (15°C at 1 bar) in kg/dm <sup>3</sup>	1057.1	DIN EN ISO 12185 :1997
Boiling range at 1 bar in °C	144.9 – 242.4	DIN EN ISO 3405 :2011
Flash point at 1 bar in °C	65.0	DIN EN ISO 2719 :2016
Cold Filter Plugging Point in °C	-40	DIN EN 116 :2018
Cloud Point in °C	-38	DIN EN 23015 :1994
Kinematic viscosity at 40°C in mm <sup>2</sup> /s	1.082	DIN EN ISO 3104 :1999
Lubricity – HFFR at 60°C in µm	320	DIN EN ISO 12156-1 :2016
Formaldehyde content in mg/kg	233	ASG 1855 Voltammetry

### Properties of the test engine

Table 2. Properties of the test engine MAN D2676LF51. The injectors in OME operation have a higher nozzle flow rate to reduce the combustion duration at high-load points.

Number of cylinders	6 (inline)
Displacement	12,419 cm <sup>3</sup>
Bore	126 mm
Stroke	166 mm
Power	294 kW
Compression ratio	18 : 1
Number of valves per cylinder	4 (2 inlet / 2 exhaust)
Charge	Two-stage waste-gate turbocharger
Exhaust gas recirculation	High-pressure & cooled
Injection system	Common Rail (max. 1800 bar)
Hydraulic nozzle flow rate	Diesel: 1,300 cm <sup>3</sup> / 30 s (at 100 bar) OME: 1,835 cm <sup>3</sup> / 30 s (at 100 bar)



## Chronological order of test runs

Table 4. Chronological order of the test runs and the respective setup. (\*) marks the last test run of the day, with the next test run happening on another day. (\*\*) The test runs of WHSC and WHTC with DPF happened between the cleaning process after the fuel change and the removal of the DPF.

Chronological order	Removal of volatile fraction		Dilution		Sampling point		Urea dosing	
	With CS	w/o CS	One-stage	Two-stage	Raw exhaust	Tailpipe	With dosing	w/o dosing
Comparison between diesel and OME: raw exhaust								
1	X			X	X			X
2		X		X	X			X
Change from diesel to OME; change of the injectors; removal of the DPF (**); cleaning of the impactor								
3	X			X	X			X
4		X		X	X			X
Investigation on OME: one-stage dilution								
5	X		X		X			X
6 (*)		X	X		X			X
7	X		X			X		X
8		X	X			X		X
Investigation on urea dosing								
9	X		X			X	X	

## Step sizes of the DMA

6.38 nm	21.7 nm	73.7 nm
6.61 nm	22.5 nm	76.4 nm
6.85 nm	23.3 nm	79.1 nm
7.10 nm	24.1 nm	82.0 nm
7.37 nm	25.0 nm	85.1 nm
7.64 nm	25.9 nm	88.2 nm
7.91 nm	26.9 nm	91.4 nm
8.20 nm	27.9 nm	94.7 nm
8.51 nm	28.9 nm	98.2 nm
8.82 nm	30.0 nm	101.8 nm
9.14 nm	31.1 nm	105.5 nm
9.47 nm	32.2 nm	109.4 nm
9.82 nm	33.4 nm	113.4 nm
10.2 nm	34.6 nm	117.6 nm
10.6 nm	35.9 nm	121.9 nm
10.9 nm	37.2 nm	126.3 nm
11.3 nm	38.5 nm	131.0 nm
11.8 nm	40.0 nm	135.8 nm
12.2 nm	41.4 nm	140.7 nm
12.6 nm	42.9 nm	145.9 nm
13.1 nm	44.5 nm	151.2 nm
13.6 nm	46.1 nm	156.8 nm
14.1 nm	47.8 nm	162.5 nm
14.6 nm	49.6 nm	168.5 nm
15.1 nm	51.4 nm	174.7 nm
15.7 nm	53.3 nm	181.1 nm
16.3 nm	55.2 nm	187.7 nm
16.8 nm	57.3 nm	194.6 nm
17.5 nm	59.4 nm	201.7 nm
18.1 nm	61.5 nm	209.1 nm
18.8 nm	63.8 nm	216.7 nm
19.5 nm	66.1 nm	224.7 nm
20.2 nm	68.5 nm	
20.9 nm	71.0 nm	

## Calculation of particle losses†

### Maximum tube Reynolds number and maximum particle Reynolds number (according to Hinds (1))

The following calculations describe the respective maximum or minimum of each value and therefore enable the decision of whether the flow is laminar or turbulent.

Temperature T:	293.15 K
Pressure p:	101.3 kPa
Tube diameter $d_t$ :	0.006 m
Air velocity $v_a$ :	5.895 m/s
Particle diameter $d_p$ :	0.23 $\mu\text{m}$
Particle velocity $v_p$ :	5.895 m/s

Air density  $\rho_a$ :

$$\rho_a = 1.293 \cdot \frac{273.15}{T} \cdot \frac{p}{101.3} = 1.2048 \frac{\text{kg}}{\text{m}^3}$$

Air dynamic viscosity  $\mu_a$ :

$$\begin{aligned} \mu_a &= 0.0000178 \cdot \left( \frac{T}{273.15} \right)^{1.5} \cdot \frac{393.396}{T + 120.246} \\ &= 1.8071 \cdot 10^{-5} \text{Pa} \cdot \text{s} \end{aligned}$$

Particle Reynolds number  $Re_p$ :

$$Re_p = 0.000001 \cdot \rho_a \cdot d_p \cdot \frac{v_p}{\mu_a} = 0.0904$$

According to Hinds, the flow is laminar for  $Re_p < 0.1$ .

Tube Reynolds number  $Re_t$ :

$$Re_t = \rho_a \cdot d_t \cdot \frac{v_a}{\mu_a} = 2358$$

According to Hinds, the flow is laminar for  $Re_t < 2000$ , but not turbulent as long as  $Re_t < 4000$  (1).

Since  $Re_p$  decreases for smaller particles and higher aerosol temperature, and  $Re_t$  decreases with higher aerosol temperature, the assumption of laminar flow in all parts of the sampling system is valid.

### Gravitational settling in the inlet (according to Willeke & Baron(2))

The following calculations describe the respective maximum or minimum of each value and therefore lead to the minimum penetration rate through the inlet.

Air dynamic viscosity $\mu_a$ :	1.8071·10 <sup>-5</sup> Pa·s
Tube diameter $d_t$ :	0.006 m
Air velocity $v_a$ :	5.895 m/s
Particle diameter $d_p$ :	0.23 $\mu\text{m}$
Particle density $\rho_p$ :	1000 kg/m <sup>3</sup>
Inlet length $l_i$ :	0.3 m
Sampling angle $\theta$ :	45°
Velocity ratio R:	1 (isokinetic)
Flow Reynolds number $Re_f$ :	2358

Slip correction factor S:

$$S = 1 + \left( \frac{2}{p \cdot d_p \cdot 0.752} \right) \cdot 6.32 + 2.01 \cdot e^{(-0.1095 \cdot p \cdot 0.752 \cdot d_p)} = 1.7551$$

Setting velocity  $v_s$ :

$$v_s = \rho_p \cdot d_p^2 \cdot 0.000000000001 \cdot 9.81 \cdot \frac{S}{18 \cdot \mu_a} = 2.8 \cdot 10^{-6} \frac{\text{m}}{\text{s}}$$

Stokes number St:

$$St = \rho_p \cdot d_p^2 \cdot 0.000000000001 \cdot \frac{S}{18 \cdot \mu_a} \cdot v_a \cdot \frac{R}{d_t} = 0.0003$$

Gravitational deposition parameter  $g_d$ :

$$g_d = l_i \cdot \frac{v_s}{v_a \cdot d_t}$$

$K(\theta)$ :

$$K(\theta) = \sqrt{g_d \cdot St} \cdot Re_t^{-0.25} \cdot \sqrt{\cos\left(\theta \cdot \frac{\pi}{180}\right)}$$

Penetration rate  $r_p$ :

$$r_p = e^{-(4.7 \cdot K(\theta)^{0.75})} = 0.9992$$

Since  $r_p$  increases for smaller particles and higher aerosol temperature, the neglect of gravitational settling in the inlet is valid.

†The calculations were performed using Matlab R2019b. Therefore it used more digits than indicated in this document. The EXCEL-Tool "aerocalc" by Paul Baron was used for the specific formulas.

### Sedimentation (according to Willeke & Baron (2))

The following calculations describe the respective maximum or minimum of each value and therefore lead to the minimum penetration rate inside the tubing.

Particle diameter $d_p$ :	0.23 $\mu\text{m}$
Particle density $\rho_p$ :	1000 $\text{kg}/\text{m}^3$
Tube diameter $d_t$ :	0.006 m
Tube length $l_t$ :	4.37 m
Incline angle $\delta$ :	0°
Mean flow velocity $v_a$ :	5.895 m/s
Flow Reynolds number $Re_f$ :	2358
Slip correction factor S:	1.7551 (for $d_p = 0.23 \mu\text{m}$ )
Setting velocity $v_s$ :	$2.8 \cdot 10^{-6}$ m/s

Intermediate number  $k_1$ :

$$k_1 = \cos\left(\pi \cdot \frac{\delta}{180}\right) \cdot 3 \cdot v_s \cdot \frac{l_t}{4 \cdot d_t \cdot v_a}$$

Intermediate number  $k_2$ :

$$k_2 = \arcsin\left(k_1^{\frac{1}{3}}\right)$$

Penetration rate  $r_p$ :

$$r_p = 1 - 2\pi \cdot \sqrt{1 - \left(k_1^{\frac{1}{3}}\right)} + k_2 - \left(k_1^{\frac{1}{3}} \cdot \sqrt{1 - k_1^{\frac{2}{3}}}\right) = 0.9996$$

Since  $r_p$  increases for smaller particles and higher aerosol temperature, the neglect of gravitational settling in the tubing is valid.

### Bent tubing (according to Willeke & Baron (2))

The following calculations describe the respective maximum or minimum of each value and therefore lead to the minimum penetration rate through bent tubing.

Particle diameter $d_p$ :	0.23 $\mu\text{m}$
Stokes number St:	0.0003
Flow Reynolds number $Re_f$ :	2358
Angle of bend $\gamma$ :	90°

Penetration rate  $r_p$ :

$$r_p = 1 - St \cdot \gamma \cdot \frac{\pi}{180} = 0.9993$$

Since  $r_p$  increases for smaller particles and higher aerosol temperature, the neglect of losses in bent tubing is valid.

### Coagulation (according to Willeke & Baron (2))

The following calculations describe the respective maximum or minimum of each value and therefore lead to the maximum coagulation rate. Furthermore, the initial particle concentration considers monodisperse aerosol of the total concentration.

Upper particle diameter $d_{pu}$ :	0.23 $\mu\text{m}$
Lower particle diameter $d_{pl}$ :	0.006 $\mu\text{m}$
Initial number concentration PN:	$10^{13}$ $1/\text{m}^3$
Coagulation coefficient c:	$5.6 \cdot 10^{-16}$ $\text{m}^3/\text{s}$
Time t:	$\sim 1$ s
(tubing length: 4.3 m, velocity: 5.9 m/s)	

Final particle concentration  $PN_f$ :

$$PN_f = \frac{PN}{1 + PN \cdot c \cdot t} = 9.9443 \cdot 10^{12} \text{ } 1/\text{m}^3$$

Final particle size  $d_{fu}$  for  $d_{pu}$ :

$$d_{fu} = d_{pu} \cdot \left(\frac{PN}{PN_{fu}}\right)^{\frac{1}{3}} = 0.2304 \mu\text{m}$$

Final particle size  $d_{fl}$  for  $d_{pl}$ :

$$d_{fl} = d_{pl} \cdot \left(\frac{PN}{PN_{fu}}\right)^{\frac{1}{3}} = 0.0060 \mu\text{m}$$

Since the aerosol is polydisperse with lower total particle concentrations and the dwell time is less than one second, the neglect of coagulation is valid.

### Thermophoretic velocity (according to Hinds (1) and Willeke & Baron (2))

The following calculations describe the respective maximum or minimum of each value and therefore lead to the maximum thermophoretic velocity tubing.

Temperature of particle $T_p$ :	693.15 K
Pressure p:	101.3 kPa
Particle diameter $d_p$ :	0.23 $\mu\text{m}$
Particle thermal conductivity $\kappa$ :	4.2 W/m·K (carbon)
Thermal gradient $\Delta T$ :	4000 K/m
Air density $\rho_{a,h}$ :	0.5095 $\text{kg}/\text{m}^3$
Air dynamic viscosity $\mu_{a,h}$ :	$3.3393 \cdot 10^{-5}$ Pa·s
Slip correction factor S:	1.7551 (for $d_p = 0.23 \mu\text{m}$ )

Mean free path  $\lambda$ :

$$\lambda = 0.000674 \cdot 0.0001 \cdot \frac{T_p}{296.15} \cdot \frac{101.3}{p} \cdot \frac{1 + \frac{110.4}{296.15}}{1 + \frac{110.4}{T_p}}$$

Intermediate factor H:

$$H = \frac{\frac{1}{1 + 6 \cdot \frac{\lambda}{d_p \cdot 0.000001}} \cdot \left(\frac{0.026}{\kappa} + 4.4 \cdot \frac{\lambda}{d_p \cdot 0.000001}\right)}{1 + 2 \cdot \frac{0.026}{\kappa} + 8.8 \cdot \frac{\lambda}{d_p \cdot 0.000001}}$$

Thermophoretic velocity  $v_T$ :

$$v_T = 3 \cdot \mu_{a,h} \cdot S \cdot H \cdot \frac{\Delta T}{2 \cdot \rho_{a,h} \cdot T_p} = 7.4375 \cdot 10^{-5} \frac{\text{m}}{\text{s}}$$

Since  $v_T$  decreases for lower aerosol temperature and lower temperature gradients, the neglect of thermophoretic losses is valid.

### Diffusional losses in a cylindrical tube-fraction passing through tube under laminar flow (according to Willeke & Baron (2))

Since the tubing length between the catalytic stripper and the SMPS is the dominant part in this calculation, the temperature inside the tubing is assumed to be 20°C. The maximum deviation in penetration efficiency between an aerosol temperature of 20°C and 220°C is less than 1.06% absolute for a particle diameter of 6 nm.

Temperature T: 293.15 K  
 Pressure p: 101.3 kPa  
 Particle diameter  $d_p$ : from 0.006  $\mu\text{m}$  to 0.23  $\mu\text{m}$   
 Tube diameter  $d_t$ : 0.006 m  
 Tube length  $l_t$ : 4.37 m  
 Air flow rate  $\dot{V}_a$ :  $1.667 \cdot 10^{-4} \text{ m}^3/\text{s}$   
 Air density  $\rho_a$ :  $1.2048 \text{ kg/m}^3$   
 Air dynamic viscosity  $\mu_a$ :  $1.8071 \cdot 10^{-5} \text{ Pa}\cdot\text{s}$   
 Slip correction factor S: depending on  $d_p$

Diffusion coefficient  $\beta$ :

$$\beta = 1.38 \cdot 10^{-23} \cdot T \cdot \frac{S}{3 \cdot \pi \cdot \mu_a \cdot d_p \cdot 0.000001}$$

$\mu_{Hinds}$ :

$$\mu_{Hinds} = \beta \cdot \frac{l_t}{\dot{V}_a}$$

Penetration rate  $r_p$ :

$$r_p = 1 - 5.5 \cdot (\mu_{Hinds})^{\frac{2}{3}} + 3.77 \cdot \mu_{Hinds}$$

### Particle losses in the ejector diluters (according to Giechaskiel et al. (3))

The transportation losses of the ejector diluters were assumed to be 5% for each diluter and for any particle diameter, according to the measurements of Giechaskiel et al. (3).

### Electrostatic losses

Transport losses due to electrostatic fields were neglected due to the usage of stainless steel wherever possible and an intermediate connection using Tygon tubing. This polymer is known as a tubing material having lower electrostatic losses than other kinds of tubing (4–6).

### Particle losses inside the catalytic stripper

The manufacturer of the catalytic stripper (Catalytic Instruments GmbH & Co. KG) provide in the manual, penetration efficiency data at nominal flow (10 l/min):

$D_p$ , nm	P						
3.00	0.01	15.70	0.55	79.10	0.73	399.50	0.75
3.11	0.01	16.30	0.56	82.00	0.73	414.20	0.75
3.22	0.02	16.80	0.57	85.10	0.74	429.40	0.75
3.34	0.02	17.50	0.58	88.20	0.74	445.10	0.75
3.46	0.03	18.10	0.58	91.40	0.74	461.40	0.75
3.59	0.04	18.80	0.59	94.70	0.74	478.30	0.75
3.72	0.05	19.50	0.60	98.20	0.74	495.80	0.75
3.85	0.05	20.20	0.60	101.80	0.74	399.50	0.75
4.00	0.07	20.90	0.61	105.50	0.74	414.20	0.75
4.14	0.08	21.70	0.62	109.40	0.74	429.40	0.75
4.29	0.09	22.50	0.62	113.40	0.74	445.10	0.75
4.45	0.10	23.30	0.63	117.60	0.74	461.40	0.75
4.61	0.11	24.10	0.64	121.90	0.74	478.30	0.75
4.78	0.13	25.00	0.64	126.30	0.74	495.80	0.75
4.96	0.14	25.90	0.65	131.00	0.74	399.50	0.75
5.14	0.16	26.90	0.65	135.80	0.74	414.20	0.75
5.33	0.17	27.90	0.66	140.70	0.74	429.40	0.75
5.52	0.19	28.90	0.66	145.90	0.74	445.10	0.75
5.73	0.21	30.00	0.67	151.20	0.74	461.40	0.75
5.94	0.22	31.10	0.67	156.80	0.74	478.30	0.75
6.15	0.24	32.20	0.68	162.50	0.74		
6.38	0.26	33.40	0.68	168.50	0.74		
6.61	0.27	34.60	0.69	174.70	0.74		
6.86	0.29	35.90	0.69	181.10	0.74		
7.11	0.30	37.20	0.69	187.70	0.74		
7.37	0.32	38.50	0.70	194.60	0.74		
7.64	0.33	40.00	0.70	201.70	0.74		
7.92	0.35	41.40	0.70	209.10	0.75		
8.21	0.36	42.90	0.70	216.70	0.75		
8.51	0.38	44.50	0.71	224.70	0.75		
8.82	0.39	46.10	0.71	232.90	0.75		
9.14	0.40	47.80	0.71	241.40	0.75		
9.48	0.42	49.60	0.71	250.30	0.75		
9.82	0.43	51.40	0.72	259.50	0.75		
10.18	0.44	53.30	0.72	269.00	0.75		
10.56	0.45	55.20	0.72	278.80	0.75		
10.94	0.46	57.30	0.72	289.00	0.75		
11.34	0.47	59.40	0.72	299.60	0.75		
11.76	0.48	61.50	0.73	310.80	0.75		
12.19	0.49	63.80	0.73	322.60	0.75		
13.10	0.51	66.10	0.73	333.80	0.75		
13.60	0.52	68.50	0.73	346.00	0.75		
14.10	0.53	71.00	0.73	358.70	0.75		
14.60	0.54	73.70	0.73	371.80	0.75		
15.10	0.54	76.40	0.73	385.40	0.75		

Figure 2 shows the calculated penetration efficiencies of the purpose-built sampling systems with and without the CS or the second dilution stage. The results of the PSD in this work use the PCRF of these calculations. Furthermore, the “Aerosol Instrument Manager” software by TSI includes the option of considering the diffusion losses inside the SMPS and a multiple charge correction. The evaluations in this study include these considerations.

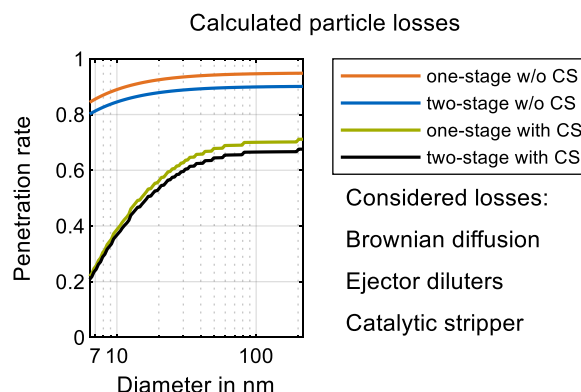


Figure 2. Calculated particle losses. The losses due to Brownian diffusion are based on calculations according to Hinds (1) with the assumption of a laminar flow inside the tubing. The losses of each ejector diluter were assumed to be 5% according to Giechaskiel et al. (3). The manufacturer of the catalytic stripper determined the respective penetration efficiency at a nominal flow rate of 10 l/min.

## References

1. Hinds WC. *Aerosol Technology: Properties, Behavior, and Measurement of Airborne Particles*. Wiley; 1999.
2. Kulkarni P, Baron PA, Willeke K. *Aerosol Measurement*. Hoboken, NJ, USA: John Wiley & Sons, Inc; 2011.
3. Giechaskiel B, Ntziachristos L, Samaras Z. Effect of ejector dilutors on measurements of automotive exhaust gas aerosol size distributions. *Meas. Sci. Technol.* 2009; 20(4):45703.
4. Liu BY, Pui DY, Rubow KL, Szymanski WW. Electrostatic effects in aerosol sampling and filtration. *Ann Occup Hyg* 1985; 29(2):251–69.
5. Tsai CS-J. Characterization of Airborne Nanoparticle Loss in Sampling Tubing. *J Occup Environ Hyg* 2015; 12(8):D161-7.
6. Asbach C, Kaminski H, Lamboy Y, Schneiderwind U, Fierz M, Todea AM. Silicone sampling tubes can cause drastic artifacts in measurements with aerosol instrumentation based on unipolar diffusion charging. *Aerosol Science and Technology* 2016; 50(12):1375–84.